PROCEEDINGS OF SPIE

SPIEDigitalLibrary.org/conference-proceedings-of-spie

Holographic techniques for recording ultrafast events

Martin Centurion, Zhiwen Liu, Gregory J. Steckman, George Panotopoulos, John H. Hong, et al.

Martin Centurion, Zhiwen Liu, Gregory J. Steckman, George Panotopoulos, John H. Hong, Demetri Psaltis, "Holographic techniques for recording ultrafast events," Proc. SPIE 4737, Holography: A Tribute to Yuri Denisyuk and Emmett Leith, (9 July 2002); doi: 10.1117/12.474957

SPIE.

Event: AeroSense 2002, 2002, Orlando, FL, United States

Holographic techniques for recording ultrafast events

Martin Centurion[a], Zhiwen Liu[b], Gregory J. Steckman[b], George Panotopoulos[b], John Hong[c], Demetri Psaltis[b]
[a]Department of Physics, California Institute of Technology; [b]Department of Electrical Engineering, California Institue of Techonology; [c]Rockwell Science Center.

ABSTRACT

In this paper we report on a holographic method used to record fast events in the nanosecond time scale. Several frames of the expansion of shock waves in air and in a polymer sample are recorded holographically in a single shot experiment, using a pulse train generated with a single pulse from a Q-switched Nd:YAG laser. The time resolution is limited by the laser pulse width, which is 5.9 ns. The different frames are recorded on the holographic material using angle multiplexing. Two cavities are used to generate the signal and reference pulses at different angles. We also present a method in which the recording material is replaced by a CCD camera. In this method the holograms are recorded directly on the CCD and digitally reconstructed. The holograms are recorded on a single frame of the CCD camera and then digitally separated and reconstructed.

Keywords: Holography, nanosecond events, shockwave, CCD hologram, pulsed hologram, single shot.

1. INTRODUCTION

Holography can be a very powerful method in the study of very fast phenomena. A well-known example is double exposure interferometry[1]. Multiple frames can be stored and reconstructed separately using multiplexing techniques. Previous work has focused on spatial multiplexing[2,3,4] where holograms are recorded at different locations of the recording medium. Pulsed holograms have also been angularly multiplexed taking advantage of the thickness of the recording medium. In one method, three lasers are used to generate three reference beams with different angles and each laser fires a pulse in a different time[5]. A rotating mirror[6] or electro-optic switches[7] have also been used to generate the reference beams. In these efforts, the speed is limited by electronics or mechanical scanning. In the systems we describe the speed is limited by the pulse width of the laser. A sequence of signal and reference pulses are incident on the recording medium. The signal pulses all travel in the same direction while the reference beam direction changes from pulse to pulse in order to angularly multiplex holograms. After the recording, a cw laser at the same wavelength is used to readout individual frames. Depending on the incidence angle, different frames can be readout separately due to the angular selectivity of the thick hologram. In the This nanosecond camera system is used to record shockwaves generated by a focused laser pulse. We also present results for a system in which the holographic recording material is replaced by a CCD camera and the holograms are stored digitally[15,16,17]. In this case all of the holograms are recorded on a single frame of the CCD camera and then separated and reconstructed digitally.

2. NANOSECOND CAMERA SYSTEM

2.1 Experimental Setup

The signal and the reference pulse trains are both generated by a single pulse from a frequency doubled Q-switched Nd:yttrium–aluminum–garnet (YAG) laser (wavelength 532 nm, pulse width 5.9 ns, energy per pulse 300 mJ, and beam diameter 9 mm). Two cavities are used to generate the signal and reference pulse trains that used to record the holograms (Fig. 1). In the signal cavity, a polarizing beam splitter is used to couple an incident pulse (which has vertical polarization) into the cavity. The Pockels cell is timed to behave like a temporary $\lambda/4$ wave plate (effectively a $\lambda/2$ wave plate since the pulse passes it twice each round trip) to rotate the polarization of the incident pulse to the horizontal direction after it first enters the cavity. It is then turned off while the pulse travels back towards the opposite mirror. The pulse is effectively trapped inside the cavity since the polarizing beam splitter transmits light with horizontal

Holography: A Tribute to Yuri Denisyuk and Emmett Leith, H. John Caulfield, Editor, Proceedings of SPIE Vol. 4737 (2002) © 2002 SPIE · 0277-786X/02/$15.00

polarization. A λ/4 wave plate is used to slightly rotate the polarization of the pulse. The induced vertically polarized component is coupled out of the cavity from the polarizing beam splitter after every round trip of the pulse.

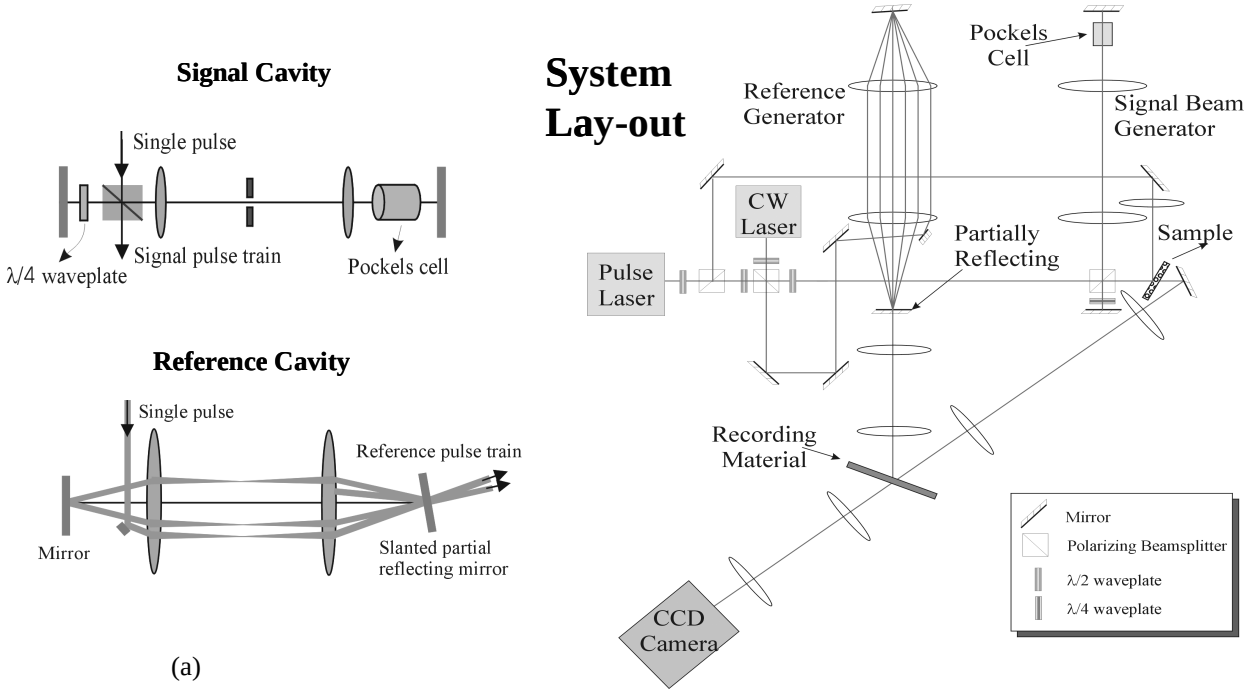

Figure 1: Holographic nanosecond camera system. (a) Signal and reference cavities. (b) System diagram.

In the reference cavity, the incident pulse enters the cavity via a small coupling mirror (Fig. 1(a)). After the coupling mirror the pulse travels as if it had originated from the center of the left mirror. The two lenses form an imaging system and the pulse hits the center of the end (right) mirror. We break the symmetry of the cavity by slanting one of the mirrors slightly. The reflected pulse then travels at a smaller angle with respect to the axis, just missing the coupling mirror. The pulse hits the center of each cavity mirror at slightly different angle after every round trip. Pulses are coupled out of the cavity by making the end mirror partially reflecting. We generate five signal and reference pulses out of a single pulse from the Nd:YAG Q-switched laser using this method. The pulse separation is about 12 ns as determined by the cavity length, which can be tuned to achieve a different pulse separation. Our current signal cavity is quite lossy due to the reflections from the optical components and the spatial filtering that is used to improve the beam profile, and thus limits us to only about five signal pulses. We recorded five plane wave pulsed holograms in the Aprilis material.[8] The diffraction efficiency of each frame and the angular selectivity curve are given in Fig. 2. The Aprilis material

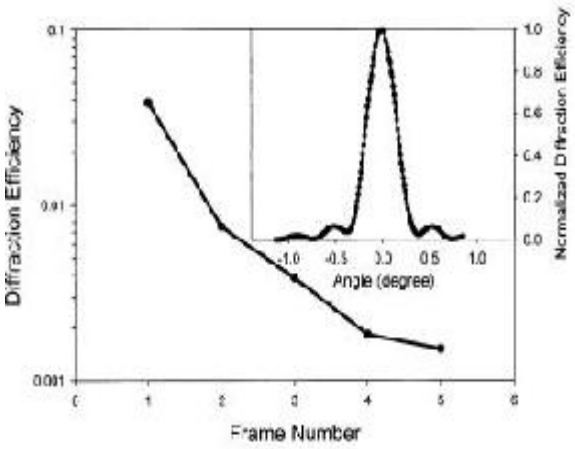

Figure 2: Diffraction efficiencies of five pulsed holograms and the selectivity curve of the first frame. Both the reference and signal pulse train have a total energy of about 37 mJ. The pulse energy in the reference and signal pulse train decays and the successively recorded holograms get weaker and weaker. Aprilis material ULSH500-7A-22 is used as the recording medium. The thickness of the material is 200 μm. The pre-exposure energy is about 2 J/cm^2 (white lamp).

yields a diffraction efficiency of approximately 1% for a 1.6 mJ/cm^2 exposure of cw illumination or a single 5.9 ns pulse. The diffraction efficiency when M holograms are superimposed goes as DE = (M/M)^2 where M/# is a material dynamic range parameter. The measured M/# of the Aprilis material is 6. Since we typically can obtain high fidelity reconstructions with DE = 10^{-4}, movies with several hundreds of frames can be recorded with an improved cavity design.

2.2 Results

The nanosecond camera system is used to record optical breakdown events. We split part of the pulse from the laser and focus it on the sample. This pumping pulse induces optical breakdown.[10,11,12,13,14] Figure 3(a) shows the optical breakdown on a poly(methylmethacrylate) (PMMA) sample. Frame I shows the plasma created by the pumping pulse.

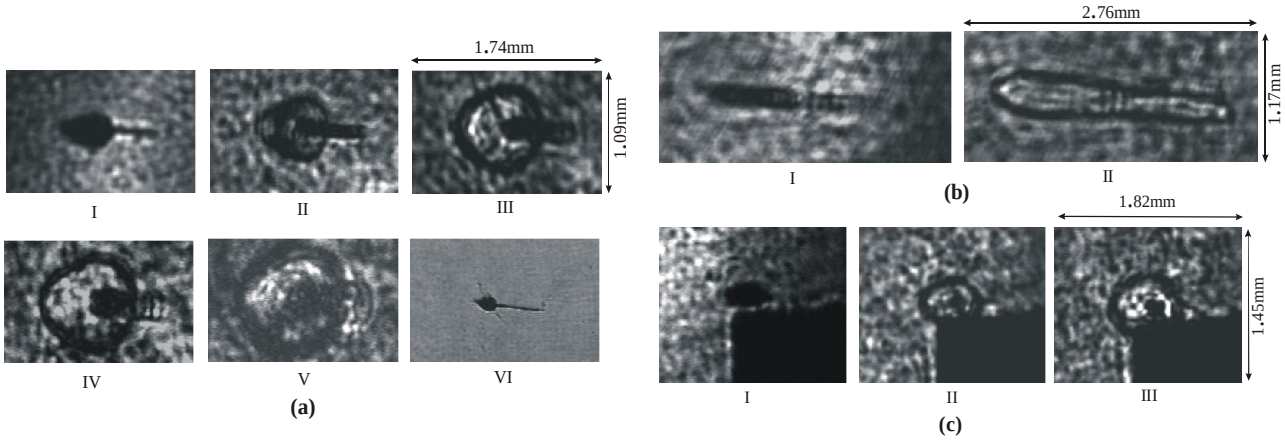

Figure 3: Optical breakdown. (a) optical breakdown in a PMMA sample. Frame I is recorded about 1ns before the pumping pulse vanishes. I,II,III,IV and V are the recorded frames with frame interval 12ns. VI is the final direct image of the sample after the optical breakdown. The intensity of the pumping beam is 1.6´1012W/cm2. (b) optical breakdown in air. The intensity of the pumping beam is 5.2´1012W/cm2. (c) optical breakdown in air with a metal blade near the focal point of the pumping beam. The intensity of the pumping beam is 1.6´1012W/cm2.

The tail is likely due to the discharge in the air in front of the sample. In frame II, a shock wave is clearly seen. The average propagating speed of the shock wave between frame I and II is about 10 km/s and that between frame IV and V is about 4 km/s. In Fig. 3(b) we show the breakdown in air. Similarly, plasma is created in frame I and soon a shock wave forms. The air discharge happens in a region near the focal point of the lens and the length of that region is about equal to the depth of focus of the lens. A line of spark is visible during the experiment. In Fig. 3(c) we focus the pumping pulse near a blade (the dark rectangular shadow). The threshold of optical breakdown is lowered dramatically by the presence of the metal blade. The optical breakdown happens mainly at a small region around the focal point which is close to the metal and produce a more spherical shock wave.

We also focus two pumping beams on PMMA and generate two shock waves as shown in Fig. 4. In (a) the lower pumping pulse has higher energy as we can see from the plasma size in frame I. When the two shock waves meet, the one with higher pressure penetrates as shown in frame III. In (b) the two shock waves roughly have the same pressure, they balance with each other in the middle.

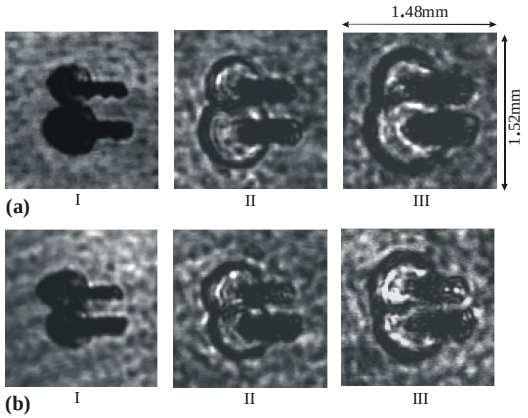

Figure 4: Interaction of two shock waves. (a) unbalanced double shock waves. (b) equal intensity waves.

A unique feature of the holographic recording is that it records the field and thus has both amplitude and phase information. We interfere the second frame of an air discharge event with the reference (a plane wave). The fringes are shown in Fig. 5(a). Apparently, the refractive index inside the region surrounded by the shock front is different from that of the outside, and there is an index gradient. In the holographic reconstruction we can focus at different depths since the object field is reconstructed. In Fig. 5(b) the plasma created on the PMMA sample is in focus while in Fig. 5(c) the shock wave due to the discharge in the air (in front of the sample) comes to focus by changing the position of the charge coupled device camera.

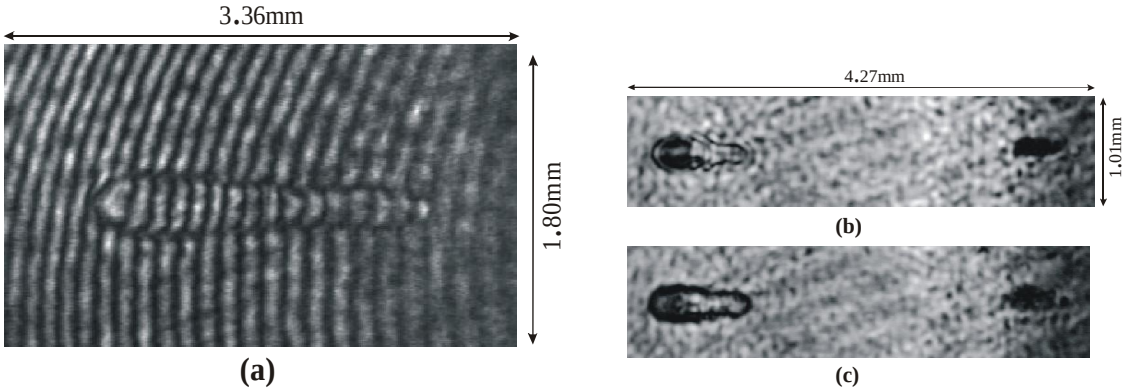

Figure 5 Holographic reconstruction of the object field. (a) Interference between a reconstructed frame and its reference wave. (b) and (c) focusing at different depths. The angle between the pumping beam and the signal beam is about 20 degrees. The pumping pulse is focused at about 1 cm in front of the PMMA sample which is consistent with the measured image depth position difference between (b) and (c).

3. DIGITAL RECORDING

3.1 Experimental Setup

The experimental setup (Fig. 6) is similar to the one described before. In fact, we use the same signal cavity to generate a sequence of pulses traveling at different angles. The difference is that now instead of two separate cavities we use only one, and use a beam splitter to divide the pulse train from the cavity into signal and reference pulses. Three pulses are generated in the cavity and imaged at the object position. The object is an air discharge created by a focused laser pulse. After going through the beam splitter the pulses are steered individually using three pairs of mirror. These pulses are recombined in a beam splitter just before hitting the CCD camera (Pulnix TM-7EX, 30 frames per second, 768 x 494 pixels, pixel size 8.4 x 9.8 μm). Three holograms are recorded on a single frame of the CCD camera, which can later be separated digitally. The resolution of the holograms is given by the pulse width, and the frame interval is given by the separation between the cavity mirrors.

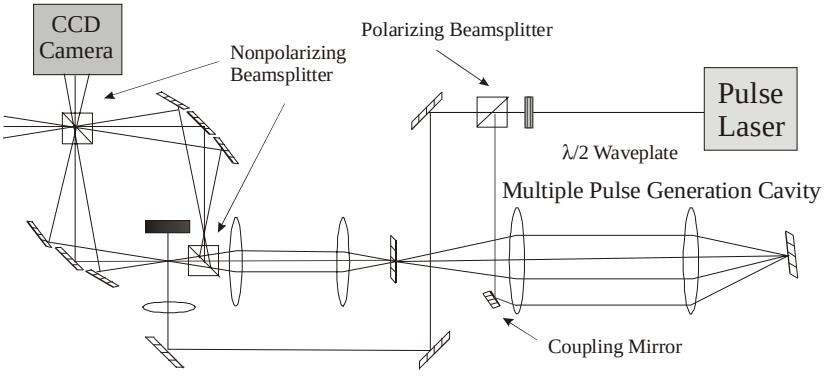

Figure 6. Setup for the nanosecond camera with digital recording.

3.2 Recording and reconstruction of digital holograms

Successive holograms are recorded on a CCD camera with a slightly different reference angle as in angular multiplexing. The resolution of the CCD camera is typically about 10 μm, therefore a small angle is between the signal and reference pulses is necessary in order to resolve the interference fringes. A beam-splitter is used in order to record holograms in Mach-Zehnder interferometer configuration. The CCD camera records the integration of the whole sequence of pulse exposure. All of the holograms are superimposed in one composite CCD frame and each can be independently reconstructed through digital spatial filtering if the image bandwidth of each hologram is sufficiently low. Individual holograms can then be filtered out and reconstructed by first performing a digital Fourier Transform on the composite image, filtering a selected pass-band corresponding to the desired hologram and then performing an inverse Fourier transform on the filtered result. In general, the recorded pattern on the CCD is proportional to

$$I = |R+S|^2 = |R|^2 + |S|^2 + R^*S + RS^* \qquad (1)$$

where R is the plane wave reference and S is the signal. There are two side bands, which correspond to the last two terms of equation 1. The position of the side band is determined by the interference pattern frequency or the carrier frequency, which can be changed by changing the reference beam incidence angle. We filter out one side band and perform the Inverse Fourier Transform. Either R*S or RS* is obtained. By taking the amplitude, the signal |S| is reconstructed. Different holograms can be recorded without overlapping with each other in the frequency domain if the reference beam angle or the carrier frequency of each hologram is different.

We can demonstrate the method by recording plane wave images (no object was present). Figure 7(a) shows the interference pattern recorded using three pairs of pulses. The three pulses are made to interfere at different angles using the steering mirror. The holograms are recorded in a single frame of the CCD camera, but they are separated in frequency space, as shown in Figure 7(b).

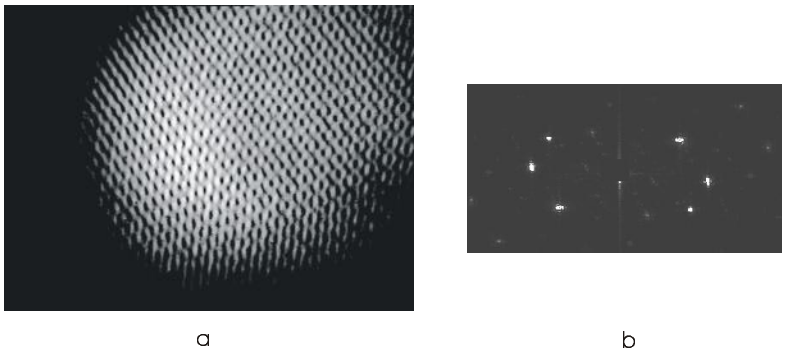

Figure 7 Digitally stored plane wave hologram. (a) Interference fringes generated by three pairs of pulses. (b) The holograms are separated in frequency space.

3.3 Results

A movie of an air discharge was recorded by focusing a pump pulse in the path of the signal pulses. The interference fringes and the Fourier transform are shown in Figure 8. After applying a filter the images are reconstructed separately. Three frames were recorded (Fig. 9(a-c). The first frame shows the plasma generated by the pump, and the next two frames show the shockwave expansion. The holograms are recorded in the far field, however, holography allows us to record both the amplitude and phase of the light, so the diffraction undergone by the object can be compensated digitally[18,19]. In figure 9(d-f) we show the images compensated for diffraction.

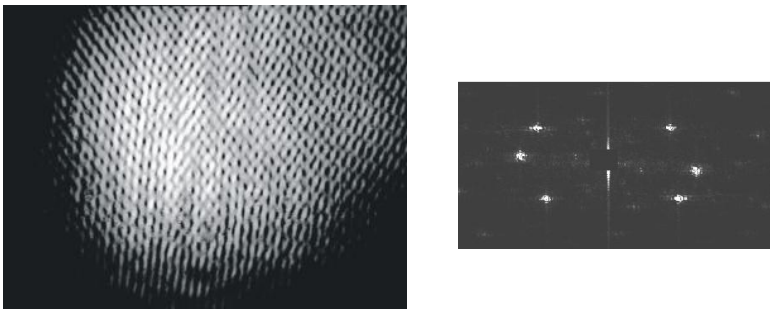

Figure 8 Digitally stored hologram of an air discharge event. (a) Interference fringes generated by three pairs of pulses. (b) The holograms are separated in frequency space.

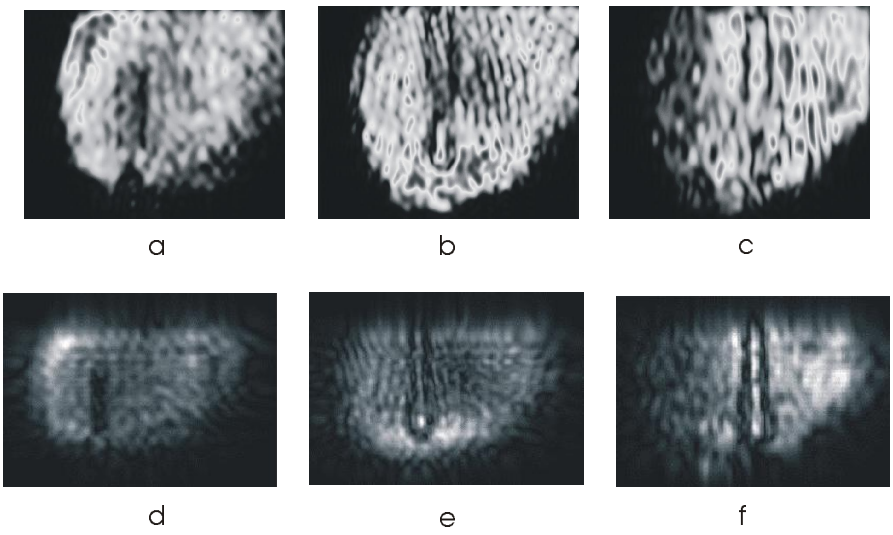

Figure 9 (a-c) The three digital image reconstructions. (d-f) The reconstructed images after diffraction compensation.

4. CONCLUSION

We have demonstrated a system to record events in nanosecond time scales. Several frames of plasma and shock wave propagation were recorded on a holographic material. We also presented a system in which the holograms can be recorded digitally. This method can also be used to record phenomena in the picosecond time scale if shorter pulses are used.

AKNOWLEDGEMENTS

This work is supported by the Air Force Office of Scientific Research and the NSF Neuromorphic Engineering Research Center.

REFERENCES

1. L.O. Heflinger, R.F. Wuerker, R.E. Brooks, *J. Appl. Phys*. **37**, 642 (1966).
2. T. Tschudi, C. Yamanaka, T. Sasaki, K. Yoshida, and K. Tanaka, *J. Phys.* D **11**, 177-180 (1978).
3. M.J. Ehrlich, J.S. Steckenrider, J.W. Wagner, *Appl. Opt*. **31**, 5947-5951 (1992).
4. W. Hentschel, W. Lauterborn, *Opt. Eng*. **24**, 687-691 (1985).
5. S. Suzuki, Y. Nozaki, H. Kimura, *Appl. Opt*. **36**, 7224-7233 (1997).
6. R.G. Racca, J.M. Dewey, *Appl. Opt*. **28,** 3652-3656 (1989).
7. R.G. Racca, J.M. Dewey, *Optics and Laser Technology* **22**, 199-204 (1990).
8. H.J. Coufal, D. Psaltis, G.T. Sincerbox (eds.), *Holographic Data Storage* (Springer, Berlin, 2000), pp.171-197.
9. F.H. Mok, G.W. Burr, D. Psaltis, *Opt. Lett*. **21**, 896-898 (1996).
10. Y.P. Raizer, *Laser-induced Discharge Phenomena* (Consultants Bureau, New York, 1977).
11. R.M. Wood, *Laser Damage in Optical Materials* (Adam Hilger, Bristol and Boston, 1986).
12. Y.R. Shen, *The Principles of Nonlinear Optics* (John Wiley & Sons, New York, 1984).
13. H. Sobral, M. Villagran-Muniz, R. Navarro-Gonzalez, A.C. Raga, *Appl. Phys. Lett*. **77**, 3158-3160 (2000).
14. Y. Tomita, M. Tsubota, K. Nagane, N. An-naka, *J. Appl. Phys*. **88**, 5993-6001 (2000).
15. E. Cuche, F. Bevilacqua, and C. Depeursinge, *Opt. Lett*. **24**, 291-293 (1999).
16. G. Indebetouw and P. Klysubun, *Appl. Phys. Lett*. **75**, 2017-2019 (1999).
17. S. Schedin, G. Pedrini, H.J. Tiziani, A.K. Aggarwal, and M.E. Gusev, *Appl. Opt*. **40**, 100-103 (2001).
18. J. Goodman, Introduction to Fourier Optics (McGraw-Hill, New York, 1996).
19. Z. Liu, M. Centurion, G. Panotopoulos, J. Hong, D. Psaltis, *Opt. Lett*, **27**, 22-24 (2002).